



LJMU Research Online

Pataky, TC, Robinson, MA and Vanrenterghem, J

Region-of-interest analyses of one-dimensional biomechanical trajectories: bridging 0D and 1D theory, augmenting statistical power.

<http://researchonline.ljmu.ac.uk/id/eprint/4852/>

Article

Citation (please note it is advisable to refer to the publisher's version if you intend to cite from this work)

Pataky, TC, Robinson, MA and Vanrenterghem, J (2016) Region-of-interest analyses of one-dimensional biomechanical trajectories: bridging 0D and 1D theory, augmenting statistical power. PeerJ, 4. ISSN 2167-8359

LJMU has developed **LJMU Research Online** for users to access the research output of the University more effectively. Copyright © and Moral Rights for the papers on this site are retained by the individual authors and/or other copyright owners. Users may download and/or print one copy of any article(s) in LJMU Research Online to facilitate their private study or for non-commercial research. You may not engage in further distribution of the material or use it for any profit-making activities or any commercial gain.

The version presented here may differ from the published version or from the version of the record. Please see the repository URL above for details on accessing the published version and note that access may require a subscription.

For more information please contact researchonline@ljmu.ac.uk

<http://researchonline.ljmu.ac.uk/>



Region-of-interest analyses of one-dimensional biomechanical trajectories: bridging 0D and 1D theory, augmenting statistical power

Todd C. Pataky¹, Mark A. Robinson² and Jos Vanrenterghem³

¹Institute for Fiber Engineering, Department of Bioengineering, Shinshu University, Ueda, Nagano, Japan

²Research Institute for Sport and Exercise Sciences, Liverpool John Moores University, Liverpool, United Kingdom

³Department of Rehabilitation Sciences, Katholieke Universiteit Leuven, Belgium

ABSTRACT

One-dimensional (1D) kinematic, force, and EMG trajectories are often analyzed using zero-dimensional (0D) metrics like local extrema. Recently whole-trajectory 1D methods have emerged in the literature as alternatives. Since 0D and 1D methods can yield qualitatively different results, the two approaches may appear to be theoretically distinct. The purposes of this paper were (a) to clarify that 0D and 1D approaches are actually just special cases of a more general region-of-interest (ROI) analysis framework, and (b) to demonstrate how ROIs can augment statistical power. We first simulated millions of smooth, random 1D datasets to validate theoretical predictions of the 0D, 1D and ROI approaches and to emphasize how ROIs provide a continuous bridge between 0D and 1D results. We then analyzed a variety of public datasets to demonstrate potential effects of ROIs on biomechanical conclusions. Results showed, first, that *a priori* ROI particulars can qualitatively affect the biomechanical conclusions that emerge from analyses and, second, that ROIs derived from exploratory/pilot analyses can detect smaller biomechanical effects than are detectable using full 1D methods. We recommend regarding ROIs, like data filtering particulars and Type I error rate, as parameters which can affect hypothesis testing results, and thus as sensitivity analysis tools to ensure arbitrary decisions do not influence scientific interpretations. Last, we describe open-source Python and MATLAB implementations of 1D ROI analysis for arbitrary experimental designs ranging from one-sample *t* tests to MANOVA.

Submitted 13 July 2016
Accepted 4 October 2016
Published 2 November 2016

Corresponding author
Todd C. Pataky,
tpataky@shinshu-u.ac.jp

Academic editor
John Hutchinson

Additional Information and
Declarations can be found on
page 10

DOI 10.7717/peerj.2652

© Copyright
2016 Pataky et al.

Distributed under
Creative Commons CC-BY 4.0

OPEN ACCESS

Subjects Animal Behavior, Bioengineering, Kinesiology, Statistics

Keywords Time series analysis, Kinematics, Constrained hypotheses, Statistical parametric mapping, Dynamics, Random field theory, Hypothesis testing, Biomechanics, Human movement

INTRODUCTION

Many biomechanical measurements may be regarded as '*n*-dimensional *m*-dimensional' (*nDmD*) continua, where *n* and *m* are the dimensionalities of the measurement domain and dependent variable, respectively. Common examples include: joint flexion (1D1D), ground reaction force (1D3D), plantar pressure distribution (2D1D) and bone strain tensor distributions (3D6D). These data are often analyzed using 0D1D metrics from regions of

interest (ROIs) which summarize particular continuum features. In this paper ‘ROI’ refers to a geometrical subset of a continuum dataset, and ‘ROI analysis’ refers to the analysis of data extracted from an ROI. More explicit definitions for these terms with literature context are provided in [Appendix A](#).

In $n > 1$ datasets ROIs are often explicitly constructed based on anatomical rationale, especially for plantar pressure ([Cavanagh & Ulbrecht, 1994](#)) and finite element analyses ([Radcliffe & Taylor, 2007](#)). In $n = 1$ datasets ROIs tend to be used both explicitly (e.g., with phase labels including: “early stance,” “push off,” “swing,” etc.) ([Blanc et al., 1999](#)) and implicitly (e.g., local extrema are used without explicitly labeled continuum regions) ([Cavanagh & Lafortune, 1980](#)). Regardless, the ultimately analyzed metrics are often $n = 0$ scalars, so we refer to this class of methods as ‘0D.’ For simplicity the remainder of this paper focusses on $n = 1$ datasets and corresponding ‘1D methods’ ([Appendix A](#)).

Recently a variety of 1D methodologies have emerged in the Biomechanics literature including functional data analysis (FDA) ([Ramsay & Silverman, 2005](#)), principal component analysis (PCA) ([Daffertshofer et al., 2004](#)) and statistical parametric mapping (SPM) ([Pataky, Robinson & Vanrenterghem, 2013](#)), each of which afford whole-field 1DmD analysis. SPM in particular is ideal for ROI-related hypothesis testing because it is valid for arbitrary 1D geometries including broken or segmented regions of arbitrary size ([Pataky, 2016](#)). FDA is less ideal because it employs continuous basis functions and not, to our knowledge, piecewise continuous ones. PCA can easily handle arbitrary ROI data, but it is predominantly a data reduction technique and not a hypothesis testing technique.

This paper therefore focusses on SPM, a methodology that was initially developed in the Neuroimaging literature in the 1990s ([Friston et al., 1995](#)), that spread to Electrophysiology through the 2000s ([Kiebel & Friston, 2004](#); [Kilner, Kiebel & Friston, 2005](#)), and which has more recently appeared in the Biomechanics literature ([Pataky, 2012](#); [Pataky, Robinson & Vanrenterghem, 2013](#)). In Neuroimaging and Electrophysiology SPM has grown into a comprehensive suite of techniques capable of handling all aspects of n -dimensional continuum analysis including univariate and multivariate continuum analysis, parametric and non-parametric probability density utilization, classical and Bayesian inference, and multi-modal analysis among other functionality ([Friston et al., 2007](#)). In the context of this paper, SPM’s classical hypothesis testing ability is key. Briefly, and considering only 1D data, SPM first computes a 1D test statistic continuum (often the t statistic continuum) from a set of experimentally measured 1D continua. This step is effectively equivalent to 1D mean and standard deviation continuum computation, which is frequently done in the Biomechanics literature. SPM then conducts statistical inference at a Type I error rate of α by calculating the critical test statistic value above which random test statistic continua (generated by smooth, 1D Gaussian continua) would traverse in only $(1 - \alpha)\%$ of an infinite number of identical experiments; if the experimentally observed continuum exceeds that critical value the null hypothesis is rejected. This general approach to classical hypothesis testing has been validated extensively in the Neuroimaging literature for 3D (and 4D) continua ([Friston et al., 1995](#); [Friston et al., 2007](#)) and has also been validated for 1D univariate and multivariate data ([Pataky, 2016](#)).

Despite the validity of 1D approaches, a variety of conceptual difficulties may arise when attempting to corroborate 0D and 1D approaches. In particular, 0D statistical results are typically tabulated using single numbers for the test statistic and p values, so test statistic continua may appear odd. Another apparent discrepancy between 0D and 1D techniques is that the former requires continuum summary metric extraction but the latter does not, so 0D techniques may appear to be somewhat more subjective than 1D techniques. A final discrepancy is that 1D techniques involve multiple comparison corrections, so they may appear to be less powerful than 0D techniques. All of these real or perceived discrepancies could lead one to infer that 0D and 1D approaches are fundamentally different.

The primary purpose of this paper was to clarify the theoretical consistency between 0D and 1D techniques as special cases of ROI analysis. To that end we describe 1D ROI theory then validate its predictions using numerical simulations of random datasets with temporal scopes ranging from single points to large 1D continua. The second purpose was to demonstrate how ROIs can be used to augment statistical power in both exploratory and hypothesis-driven experiments. The final purpose was to introduce an open-source software implementation of ROI analysis (in [Appendix C](#)) which emphasizes how 0D, 1D and ROI analyses can all be executed using a common software interface.

METHODS

All analyses were implemented in Python 2.7 ([Van Rossum, 2014](#)) using Canopy 1.6 (Enthought Inc., Austin, TX, USA) and spm1d ([Pataky, 2012](#); [Pataky, 2016](#)) (<http://www.spm1d.org>). All datasets described below are included in the **spm1d** package and are accessible using the **spm1d.data** interface as described in [Appendix D](#). High-level Python and MATLAB (The MathWorks, Natick, MA, USA) interfaces for ROI analyses are now available in spm1d as described in [Appendix C](#).

ROI theory and validation

In classical hypothesis testing the null hypothesis is rejected if the experimentally observed test statistic t exceeds a critical threshold t^* , which can be computed according to:

$$P(t > t^*) = \alpha \quad (1)$$

where α is the Type I error rate (usually 0.05) and $P(t > t^*)$ is the probability that the test statistic exceeds t^* if the null hypothesis is true.

For an ROI of size S ($S \geq 0$), [Eq. \(1\)](#) can be written as ([Friston et al., 2007](#); [Pataky, 2016](#)):

$$P(t_{\max} > t^*) = 1 - \exp \left[-P_{0D}(t > t^*) - \frac{S}{W} \frac{\sqrt{4 \log 2}}{2\pi} \left(1 + \frac{(t^*)^2}{\nu} \right)^{-(\nu-1)/2} \right] = \alpha \quad (2)$$

where t_{\max} is the maximum value of the t statistic inside the ROI, $P_{0D}(t > t^*)$ is the probability under the null hypothesis that 0D random Gaussian data will produce a t value greater than t^* , W is the FWHM representing trajectory smoothness ([Appendix B](#)), and ν is the degrees of freedom. Note that $P(t_{\max} > t^*)$ converges to $P_{0D}(t > t^*)$ as S approaches zero, and that t^* must increase as S increases to maintain a given α . In other words, the larger the

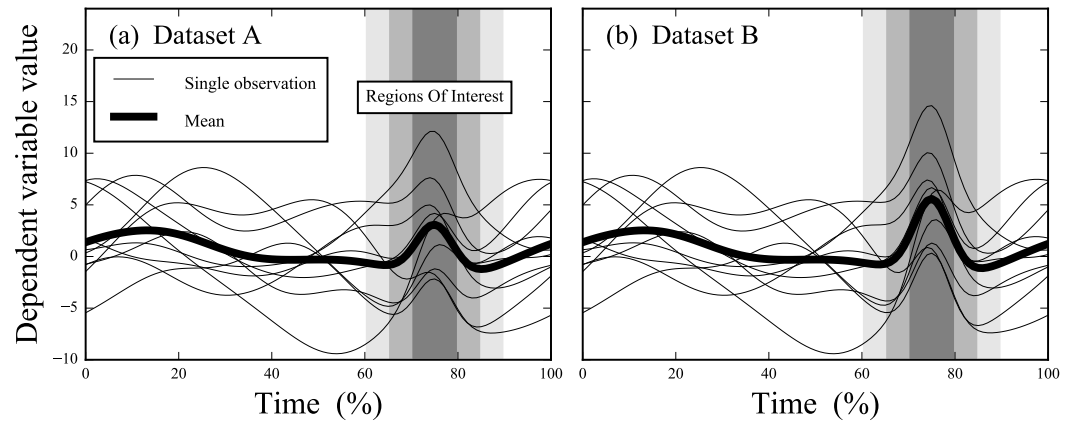


Figure 1 Simulated datasets. Datasets A and B are identical except in Dataset B the signal at time = 75% is amplified. Three regions of interest (ROIs) are depicted, centered at time = 75% and spanning time windows of 10%, 20% and 30%, respectively.

ROI, the more likely smooth, purely random 1D Gaussian data are to produce high t values. Also note that Eq. (2) can accommodate multiple ROIs using a relatively simple correction (Friston et al., 2007).

We computed t^* for a range of ROI sizes (S), smoothness values (FWHM) and sample sizes (ν). ROI size was systematically varied over the full range of possibilities (i.e., from 0 to 100% trajectory length). FWHM and ν values were selected to span a range of values observed in representative open-access biomechanical datasets (FWHM = [5, 50], ν = [5, 49]) (Pataky, Vanrenterghem & Robinson, 2016).

To validate Eq. (2) for arbitrary ROI sizes we simulated 100,000 smooth, purely random Gaussian 1D datasets using ‘rft1d’ (Pataky, 2016), and repeated for each combination of S , FWHM and ν values. For each random dataset we computed t_{\max} , thereby producing one distribution of 100,000 t_{\max} values for each combination of parameters. We then estimated t^* for each distribution as the 95th percentile of the distribution, then qualitatively compared to the theoretical result (Eq. (2)).

Example ROI analyses

Simulated datasets

Datasets A and B (Fig. 1) (Pataky, Robinson & Vanrenterghem, 2013) consisted of ten simulated, smooth, random 1D Gaussian fields to which a Gaussian pulse was added at time = 75%. The degrees of freedom and number of time nodes were $\nu = 9$ and $Q = 101$, respectively, for both datasets. The pulse was slightly larger in Dataset B than in Dataset A. Both were analyzed using six procedures, in order of increasing conservativeness: (1) 0D analyses on the local maxima at time = 75%, (2–4) 1D ROI analysis with ROIs centered at time = 75% and with temporal sizes of $\pm 5\%$, $\pm 10\%$ and $\pm 15\%$, respectively, (5) 1D full-field analysis (i.e., with ROI size = 100%), and (6) 1D full-field analysis with a Bonferroni correction. The latter assumes independence amongst adjacent trajectory nodes so is overly conservative for smooth data (Pataky, Robinson & Vanrenterghem, 2013).

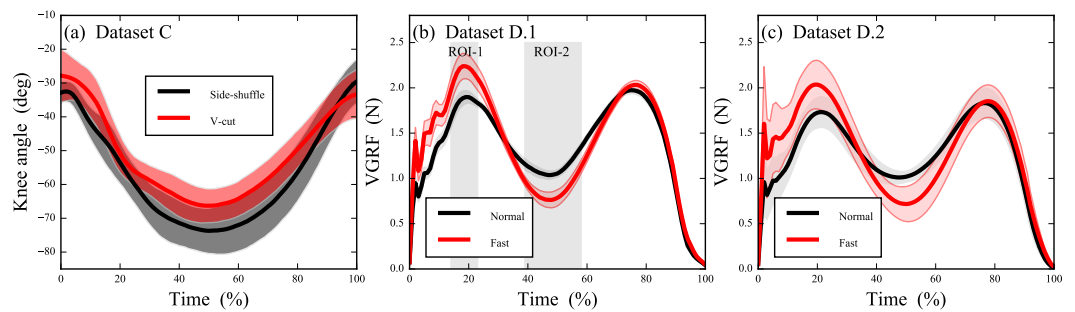


Figure 2 Experimental datasets; error clouds depict standard deviations. (A) Knee kinematics during side-shuffle and v-cut maneuvers (Neptune, Wright & Van den Bogert, 1999). (B) Pilot data from $N = 1$ subject comparing vertical ground reaction force (VGRF) in “Normal” vs. “Fast” walking (Pataky et al., 2008). (C) Subsequent identical VGRF experiment conducted on $N = 6$ subjects (Pataky et al., 2008).

Experimental datasets

Dataset C (Fig. 2A) (Neptune, Wright & Van den Bogert, 1999) ($v = 7$, $Q = 101$) contained stance-phase sagittal plane knee angles from eight participants who each performed both side-shuffle and v-cut maneuvers. We started with 0D analysis of maximal knee flexion (i.e., $S = 0$), then conducted three ROI analyses with ROIs centered approximately on maximal flexion (time = 50%) and with temporal extents of 10%, 40% and 80%, respectively. Finally, the 1D full-field ROI and Bonferroni procedures were applied as in the simulated datasets.

Dataset D (Figs. 2B and 2C) (Pataky, Robinson & Vanrenterghem, 2013) ($Q = 101$) contained stance-phase body-weight-normalized vertical ground reaction forces (VGRF) from seven subjects who each performed normal, self-paced walking and fast walking in a randomized order. Analysis proceeded in two-stages to demonstrate how ROIs can be used to increase analysis sensitivity in exploratory experiments (Pataky, Vanrenterghem & Robinson, 2016, Fig.7). First, the chronologically first subject was separated as a pilot subject (Fig. 2B). This subject’s results were examined qualitatively and were used to define ROIs. Finally, those ROIs were used as an *a priori* constraint in analysis of the six remaining subjects (Fig. 2C) ($v = 5$). Results of this ROI-driven two-stage procedure were compared to a full-field 1D analysis.

RESULTS

Critical thresholds t^* necessary to maintain $\alpha = 0.05$ (Eq. (2)) increased nonlinearly as ROI size increased and t^* values for 1D data converged to 0D t^* values as ROI size approached zero (Fig. 3). Numerical simulations validated theoretical t^* values for arbitrary 1D field smoothness values and arbitrary sample sizes. These results emphasize that 0D analyses are a special case of 1D analysis for which ROI size is zero.

In Dataset A, the test statistic exceeded the critical threshold for 0D analysis and also for a narrow ROI of 10%, but failed to reach the thresholds for wider ROIs of 20% and 30%, and also failed to reach the full-field threshold (Fig. 4A). In contrast, Dataset B’s slightly amplified signal at time = 75% exceeded all thresholds except for the highly conservative

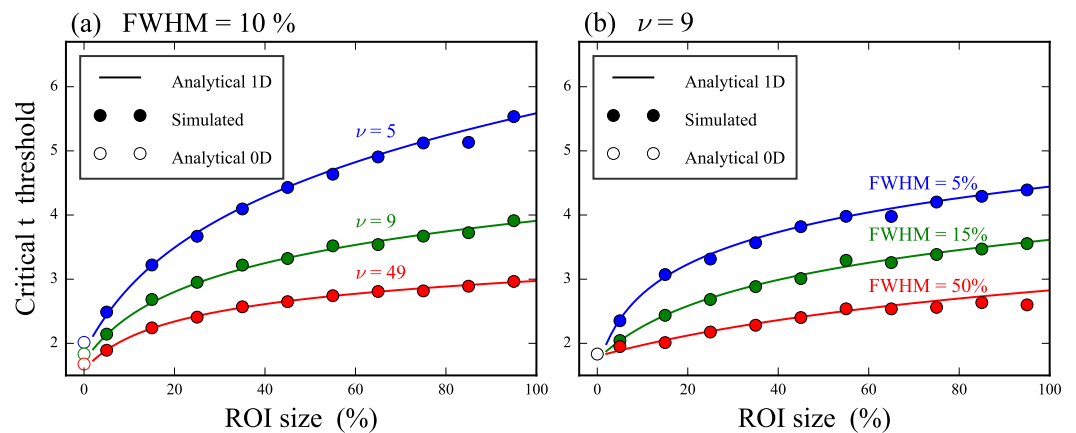


Figure 3 Validation of theoretical critical thresholds for region of interest (ROI) analysis. (A) Three different degrees of freedom (ν) and one smoothness (FWHM) value. (B) Three different FWHM values and one ν value. The analytical 0D results assume 0D Gaussian randomness and the 1D results assume smooth 1D Gaussian randomness.

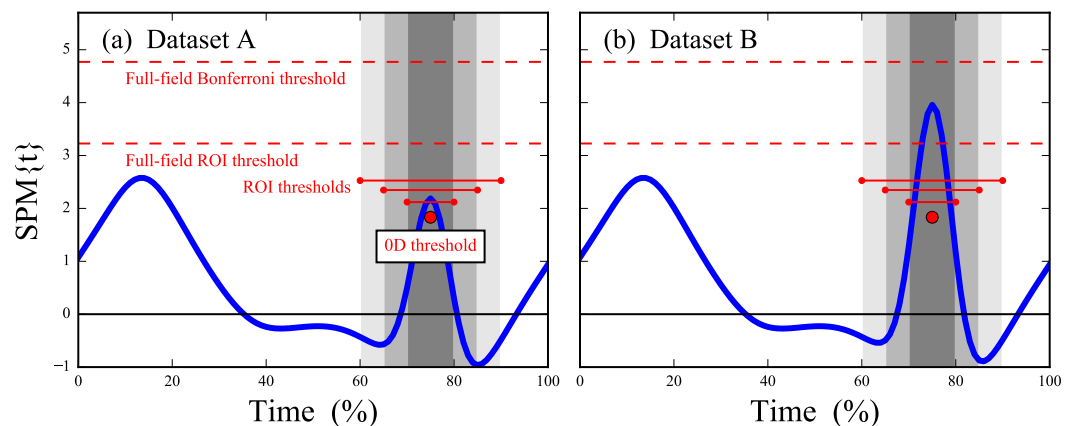


Figure 4 Simulated dataset hypothesis testing results. “SPM{t}” denotes the t value extended in time to form a ‘statistical parametric map.’ Six critical thresholds are depicted (see text). The width of each threshold depicts the temporal extent of the null hypothesis.

full-field Bonferroni correction (Fig. 4B). These results imply that small ROIs can identify relatively small effects like in Dataset A, and that large or even full-field ROIs can identify large effects. ROIs thus embody a trade-off between statistical power and the temporal scope of the null hypothesis; statistical power decreases as ROI size increases and vice versa.

For Dataset C, 0D analysis conducted on maximum knee flexion passed the critical threshold, as did a moderately broad ROI of 40% (Fig. 5). However, an ROI of 80% and full-field analysis failed to cross the critical threshold in the vicinity of maximum flexion. The null hypothesis was nevertheless rejected for both an ROI size of 80% and full-field analysis, but in this case the statistical conclusion pertains to regions other than maximum flexion.

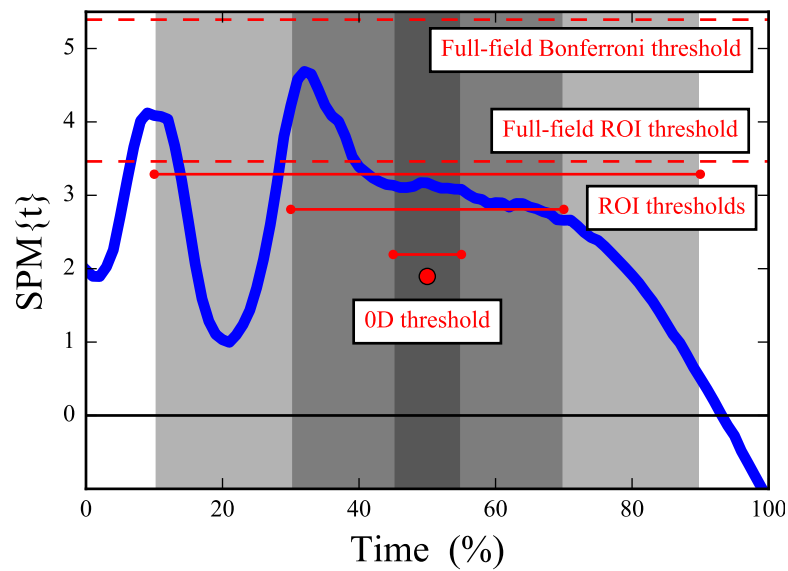


Figure 5 Dataset C (knee flexion/extension) hypothesis testing results. “ $SPM\{t\}$ ” denotes the t value. Critical thresholds are presented as in Fig. 4, with both the height and temporal extent of each threshold depicted.

For Dataset D the pilot subject’s data were used to identify two relatively narrow ROIs in the vicinity of the first local maximum and the local minimum at mid-stance (Fig. 6A). These ROIs led to null hypothesis rejection for both ROIs in the independent six-subject dataset (Fig. 6C). Had the ROIs not been defined the null hypothesis would not have been rejected (Fig. 6B).

DISCUSSION

The main purpose of this paper was to clarify the theoretical consistency between “0D” and “1D” analyses, and to emphasize that both are actually just special cases of ROI analysis. In particular, the ROI size (S) and 1D smoothness (FWHM) parameters together construct a continuous theoretical bridge between 0D and 1D methodologies (Eq. (2), Fig. 3). ROI-based statistical analysis of nD continua was formalized in the Neuroimaging literature (Brett *et al.*, 2002; Poldrack, 2006; Friston *et al.*, 2007) where established ROI software tools exist, including especially MarsBar (Hammers *et al.*, 2002; Brett *et al.*, 2002) for SPM99 (Wellcome Trust Centre for Neuroimaging, University College London, UK).

Although ROI analyses are common in biomechanical applications like plantar pressure analysis (Cavanagh & Ulbrecht, 1994) and finite element analysis (Radcliffe & Taylor, 2007), statistical ROI theory has not, to our knowledge, been addressed in the Biomechanics literature.

The key theoretical point to consider when implementing ROI analyses is that small ROIs can more readily detect true within-region effects than large ROIs (Figs. 3 and 4). However, ROI analysis are not necessarily more sensitive than full-field 1D analysis because effects may exist outside the ROI (Fig. 5, narrowest ROI). An investigator must therefore balance local signal detectability (via narrow *a priori* ROI definition) with full-field signal

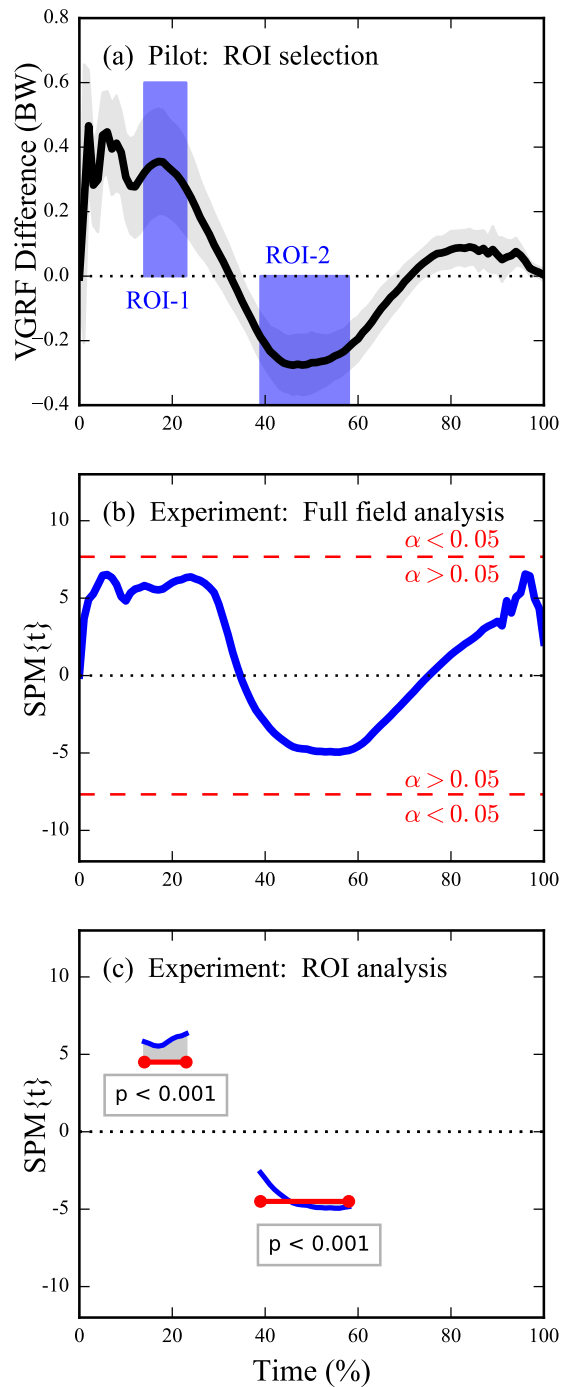


Figure 6 Dataset D (VGRF) sensitivity augmentation procedure and results. (A) Pilot study's mean inter-condition VGRF difference (see Fig. 2B) for $N = 1$ subject along with user-defined ROIs. The ROIs specify both the direction and temporal extent of an omnibus a priori hypothesis to be tested in an independent experiment. (B) Experimental analysis on $N = 6$ independent subjects using full-field inference (i.e., had no ROIs been selected); “SPM{t}” denotes the t value. The experimental differences between Normal and Fast are insufficiently large to reject the full-field null hypothesis (because the t value fails to traverse the critical threshold—depicted in red—at $\alpha = 0.05$). (C) Experimental analysis using ROI-based inference: the omnibus ROI-based null hypothesis is rejected.

detectability (via larger ROIs). In the absence of an *a priori* hypothesis regarding a specific portion of the continuum it has been suggested that full-field analyses should be conducted (Pataky, Vanrenterghem & Robinson, 2016), and this paper extends that suggestion to include a caveat for exploratory work in a two-stage procedure involving an initial full-field analysis on an exploratory dataset followed by more precise ROI-based testing (Fig. 6).

An apparent limitation of ROIs is that, since they can create / eradicate statistical significance (Figs. 4 and 5), they have the potential to be abused. We don't regard this limitation as unique to ROI analysis because ROI size, like α , can be manipulated to artificially raise / lower critical thresholds. We would therefore recommend that, instead of choosing a single ROI size or a single α , investigators should actively manipulate all parameters that might affect ultimate conclusions including: ROI size, α , data filtering, coordinate system definitions, etc., and then actively report the results of those manipulations in a sensitivity analysis as has been done elsewhere (Pataky et al., 2014). If the reported results are robust to those manipulations then one can be more confident that the reported results are neither false positives (Pataky, Vanrenterghem & Robinson, 2016) nor false negatives. Such manipulations may be especially important for biomechanical datasets considering that these data can be sensitive to ROI definitions (Figs. 5–6), and also considering that some controversies regarding the relative merits of 0D and ROI vs. full-field analysis exist in other literatures (Kubicki et al., 2002; Giuliani et al., 2005; Furutani et al., 2005; Friston et al., 2006; Saxe, Brett & Kanwisher, 2006; Snook, Plewes & Beaulieu, 2007; Kilner, 2013).

More formally, ROI definitions and procedures should be considered from the perspective of 'circular analysis' (Kriegeskorte et al., 2009), an umbrella term encompassing bias-generating factors in scientific interpretations of processed data. In particular, the approach we have recommended with Dataset D — ROI generation based on independent-subject pilot studies—is analogous to 'functional localizers' in the Neuroimaging literature for which substantial benefits but also substantial circular risks exist (Friston et al., 2006; Saxe, Brett & Kanwisher, 2006; Kilner, 2013). As a simple example of circular analysis and its dangers consider the local maximum in Dataset A near time = 15% (Fig. 4A). Defining an ROI about this maximum after seeing this result would lead to null hypothesis rejection even for relatively broad ROIs of 20%. This would be a circular conclusion because the observed result has directly affected the conclusion's assumption that the identified ROI was not of *a priori* interest but is now. In contrast, the 1D (full-field) threshold correctly fails to reject the null hypothesis; the 1D approach's conclusion is not circular because the *a priori* assumption of full-field effects was not affected by the observed result.

The literature contains a variety of recommendations regarding avoiding bias associated with circularity in ROI analyses, and recent developments in particular show that it is possible to use algorithmic data-driven ROI selection in an unbiased manner to increase statistical power and also maintain control over Type I error rates (Brooks, Zoumpoulaki & Bowman, *in press*). This result is limited to specific cases of experimental variance, but may nevertheless be promising for researchers concerned regarding inadequate power in analyses of large 1D datasets with potentially many 1D variables. Regardless, if one wishes to conduct ROI analysis or otherwise reduce the recorded 1D dataset, they should be aware

of circularity and how circular (il)logic can produce a vast array of biased conclusions following dataset reduction.

A technical point not addressed in the analyses above is how to handle within-ROI signals that extend beyond the ROI. This situation is observable in Fig. 6C, when the test statistic value is greater than the threshold on the ROI boundaries. From a classical hypothesis perspective the point is moot because the null hypothesis is rejected regardless of the temporal scope of a supra-threshold signal. It has been recommended elsewhere that, if a within-ROI signal is detected, the entire signal be reported even if it extends outside of the ROI (Friston *et al.*, 2007). Our recommended approach of manipulating ROI location and size in a sensitivity analysis is consistent with that approach in that ROI boundaries should generally be regarded as soft.

In summary, this paper has introduced and validated an ROI approach for analyzing 1D biomechanical trajectories which clarifies the consistency between common 0D approaches and recent 1D approaches. Since biomechanical interpretations can be sensitive not only to ROI size but also to other data processing particulars like filtering and coordinate system definitions, it is recommended that ROIs be used only when there is adequate *a priori* justification for ignoring other regions of the 1D continuum, and that when they are used ROI sensitivity results are also reported.

ADDITIONAL INFORMATION AND DECLARATIONS

Funding

This work was supported by Wakate A Grant 15H05360 from the Japan Society for the Promotion of Science. The funders had no role in study design, data collection and analysis, decision to publish, or preparation of the manuscript.

Grant Disclosures

The following grant information was disclosed by the authors:
Japan Society for the Promotion of Science: 15H05360.

Competing Interests

The authors declare there are no competing interests.

Author Contributions

- Todd C. Pataky conceived and designed the experiments, analyzed the data, wrote the paper, prepared figures and/or tables, reviewed drafts of the paper.
- Mark A. Robinson and Jos Vanrenterghem conceived and designed the experiments, analyzed the data, wrote the paper, reviewed drafts of the paper.

Data Availability

The following information was supplied regarding data availability:

All raw data analyzed in this paper are available in the “spm1d” software package available at: <http://www.spm1d.org>.

Supplemental Information

Supplemental information for this article can be found online at <http://dx.doi.org/10.7717/peerj.2652#supplemental-information>.

REFERENCES

- Blanc Y, Balmer C, Landis T, Vingerhoets F. 1999.** Temporal parameters and patterns of the foot roll over during walking: normative data for healthy adults. *Gait and Posture* **10(2)**:97–108.
- Brett M, Anton JL, Valabregue R, Poline JB. 2002.** Region of interest analysis using the MarsBar toolbox for SPM 99. *NeuroImage* **16(2)**:S497.
- Brooks JL, Zoumpoulaki A, Bowman H. 2016.** Data-driven region-of-interest selection without inflating Type I error rate. *Psychophysiology* in press. Available at <https://kar.kent.ac.uk/id/eprint/55323>.
- Cavanagh PR, Lafortune MA. 1980.** Ground reaction forces in distance running. *Journal of Biomechanics* **13(5)**:397–406 DOI [10.1016/0021-9290\(80\)90033-0](https://doi.org/10.1016/0021-9290(80)90033-0).
- Cavanagh PR, Ulbrecht JS. 1994.** Clinical plantar pressure measurement in diabetes: rationale and methodology. *The Foot* **4(3)**:123–135 DOI [10.1016/0958-2592\(94\)90017-5](https://doi.org/10.1016/0958-2592(94)90017-5).
- Daffertshofer A, Lamoth CJC, Meijer OG, Beek PJ. 2004.** PCA in studying coordination and variability: a tutorial. *Clinical Biomechanics* **19(4)**:415–428.
- Friston K, Holmes A, Worsley K, Poline J, Frith C, Frackowiak R. 1995.** Statistical parametric maps in functional imaging: a general linear approach. *Human Brain Mapping* **2(4)**:189–210 DOI [10.1002/hbm.460020402](https://doi.org/10.1002/hbm.460020402).
- Friston KJ, Ashburner JT, Kiebel SJ, Nichols TE, Penny WD. 2007.** Statistical parametric mapping: the analysis of functional brain images. Amsterdam: Elsevier/Academic Press.
- Friston KJ, Rotshtein P, Geng JJ, Sterzer P, Henson RN. 2006.** A critique of functional localisers. *NeuroImage* **30(4)**:1077–1087 DOI [10.1016/j.neuroimage.2005.08.012](https://doi.org/10.1016/j.neuroimage.2005.08.012).
- Furutani K, Harada M, Minato M, Morita N, Nishitani H. 2005.** Regional changes of fractional anisotropy with normal aging using statistical parametric mapping (SPM). *Journal of Medical Investigation* **52(3–4)**:186–190 DOI [10.2152/jmi.52.186](https://doi.org/10.2152/jmi.52.186).
- Giuliani NR, Calhoun VD, Pearlson GD, Francis A, Buchanan RW. 2005.** Voxel-based morphometry versus region of interest: a comparison of two methods for analyzing gray matter differences in schizophrenia. *Schizophrenia Research* **74(2–3)**:135–147 DOI [10.1016/j.schres.2004.08.019](https://doi.org/10.1016/j.schres.2004.08.019).
- Hammers A, Koepp MJ, Free SL, Brett M, Richardson MP, Labbé C, Cunningham VJ, Brooks DJ, Duncan J. 2002.** Implementation and application of a brain template for multiple volumes of interest. *Human Brain Mapping* **15(3)**:165–174 DOI [10.1002/hbm.10016](https://doi.org/10.1002/hbm.10016).
- Kiebel SJ, Friston KJ. 2004.** Statistical parametric mapping for event-related potentials (II): a hierarchical temporal model. *NeuroImage* **22(2)**:503–520 DOI [10.1016/j.neuroimage.2004.02.013](https://doi.org/10.1016/j.neuroimage.2004.02.013).

- Kilner JM. 2013.** Bias in a common EEG and MEG statistical analysis and how to avoid it. *Clinical Neurophysiology* **124**(10):2062–2063.
- Kilner JM, Kiebel SJ, Friston KJ. 2005.** Applications of random field theory to electrophysiology. *Neuroscience Letters* **374**(3):174–178 DOI [10.1016/j.neulet.2004.10.052](https://doi.org/10.1016/j.neulet.2004.10.052).
- Kriegeskorte N, Simmons WK, Bellgowan PSF, Baker CI. 2009.** Circular analysis in systems neuroscience: the dangers of double dipping. *Nature Neuroscience* **12**(5):535–540 DOI [10.1038/nn.2303](https://doi.org/10.1038/nn.2303).
- Kubicki M, Shenton ME, Salisbury DF, Hirayasu Y. 2002.** Voxel-based morphometric analysis of gray matter in first episode schizophrenia. *NeuroImage* **17**(4):1711–1719.
- Neptune RR, Wright IC, Van den Bogert AJ. 1999.** Muscle coordination and function during cutting movements. *Medicine & Science in Sports & Exercise* **31**(2):294–302.
- Pataky TC. 2012.** One-dimensional statistical parametric mapping in Python. *Computer Methods in Biomechanics and Biomedical Engineering* **15**(3):295–301 DOI [10.1080/10255842.2010.527837](https://doi.org/10.1080/10255842.2010.527837).
- Pataky TC. 2016.** RFT1D: smooth one-dimensional random field upcrossing probabilities in Python. *Journal of Statistical Software* **71**(7):i07 DOI [10.18637/jss.v071.i07](https://doi.org/10.18637/jss.v071.i07).
- Pataky TC, Caravaggi P, Savage R, Parker D, Goulermas JY, Sellers WI, Crompton RH. 2008.** New insights into the plantar pressure correlates of walking speed using pedobarographic statistical parametric mapping (pSPM). *Journal of Biomechanics* **41**(9):1987–1994.
- Pataky TC, Robinson MA, Vanrenterghem J. 2013.** Vector field statistical analysis of kinematic and force trajectories. *Journal of Biomechanics* **46**(14):2394–2401 DOI [10.1016/j.jbiomech.2013.07.031](https://doi.org/10.1016/j.jbiomech.2013.07.031).
- Pataky TC, Robinson MA, Vanrenterghem J, Savage R, Bates K, Crompton RH. 2014.** Vector field statistics for objective center-of-pressure trajectory analysis during gait, with evidence of scalar sensitivity to small coordinate system rotations. *Gait and Posture* **40**(1):255–258 DOI [10.1016/j.gaitpost.2014.01.023](https://doi.org/10.1016/j.gaitpost.2014.01.023).
- Pataky TC, Vanrenterghem J, Robinson MA. 2016.** The probability of false positives in zero-dimensional analyses of one-dimensional kinematic, force and EMG trajectories. *Journal of Biomechanics* **49**:1468–1476 DOI [10.1016/j.jbiomech.2016.03.032](https://doi.org/10.1016/j.jbiomech.2016.03.032).
- Poldrack RA. 2006.** Region of interest for fMRI. *Social Cognitive and Affective Neuroscience* **2**(1):67–70 DOI [10.1093/scan/nsm006](https://doi.org/10.1093/scan/nsm006).
- Radcliffe IAJ, Taylor M. 2007.** Investigation into the affect of cementing techniques on load transfer in the resurfaced femoral head: a multi-femur finite element analysis. *Clinical Biomechanics* **22**(4):422–430.
- Ramsay JO, Silverman BW. 2005.** *Functional data analysis*. New York: Springer.
- Saxe R, Brett M, Kanwisher N. 2006.** Divide and conquer: a defense of functional localizers. *NeuroImage* **30**(4):1088–1096 DOI [10.1016/j.neuroimage.2005.12.062](https://doi.org/10.1016/j.neuroimage.2005.12.062).
- Snook L, Plewes C, Beaulieu C. 2007.** Voxel based versus region of interest analysis in diffusion tensor imaging of neurodevelopment. *NeuroImage* **34**(1):243–252 DOI [10.1016/j.neuroimage.2006.07.021](https://doi.org/10.1016/j.neuroimage.2006.07.021).
- Van Rossum G. 2014.** The Python library reference—release 2.7.8. Python Software Foundation. Available at <https://www.python.org>.

Appendix A Nomenclature

This Appendix proposes a set of terms and definitions for use in analyses of 1D biomechanical continua (Table A.1) and relates these terms to analogous, established terms from the neuroimaging literature (Table A.2). Note that the neuroimaging terminology cannot easily be used for 1D applications because the meaning of ‘volume’ is unclear for 1D data.

Table A.1: Proposed nomenclature for statistical parametric mapping (SPM) analyses of 1D continua.

Category	Term	Abbreviation	Description
Geometry	Point of interest	POI	A single position in a 1D continuum. (e.g. time = 10%)
	Region of interest	ROI	A continuous portion of a 1D continuum. (e.g. time = 20–50%).
Statistical inference	0D inference		*Inference procedures applied to 0D univariate or multivariate data which do not account for correlation amongst adjacent continuum points.
	1D inference		Inference procedures applied to univariate or multivariate 1D data which use multiple comparisons corrections to account for correlation amongst adjacent continuum points. RFT procedures are assumed unless otherwise stated.
	Random Field Theory	RFT	Provides analytical parametric solutions for probabilities associated with smooth 1D Gaussian continua, and in particular the probability that small samples of 1D Gaussian continua will produce test statistic continua that reach certain heights in particular experiments. Reference: Adler and Taylor (2007)
	Small region correction	SRC	A multiple comparisons correction across within-ROI values using (parametric) RFT or a nonparametric alternative. RFT is assumed unless otherwise stated.

General Methodology	0D analysis		Analysis of univariate or multivariate 0D data using 0D inference procedures.
	1D analysis		Analysis of univariate or multivariate 1D data using 1D inference procedures
	0D method		A method which conducts 0D analysis of 0D data.
	1D method		A method which conducts 1D analysis of 1D data.
	Statistical Parametric Mapping	SPM	A methodology for analyzing nD continua, often using classical hypothesis testing. SPM's classical hypothesis testing involves: (i) test statistic continuum computation from a set of registered nD continua, (ii) continuum smoothness estimation based on the nD gradient of the model residuals, (iii) critical threshold computation using RFT and the estimated smoothness, and (iv) probability value computation using RFT and the estimated smoothness for threshold-surviving clusters. Reference: Friston et al. (2007)
	Region of interest analysis	ROIA	A set of procedures involving (i) ROI definition and (ii) statistical analyses of ROI data.
Specific Methodology	0D metric-based ROI analysis	ROIA-0D	ROIA which conducts 0D analysis on a 0D summary metric (e.g. mean, median, maximum, etc.) that is meant to summarize or otherwise represent all values in an ROI. ROIA-0D with a local extremum summary metric (minimum or maximum) is common in the Biomechanics literature.
	1D ROI analysis	ROIA-1D	ROIA which conducts 1D analysis of an ROI's data using a small region correction (SRC). This is the focus of the main manuscript. Equivalent to 'SRC-based ROI analysis'.

*Note: Bonferroni and other corrections applied across multiple continuum nodes but which do not consider inter-node correlation are included in '0D inference'.

Table A.2: Relevant nomenclature from the neuroimaging literature. Terms without abbreviations do not explicitly appear in the literature and are instead introduced here to clarify connections to the proposed nomenclature in Table A.1.

Term	Abbreviation	Description
Region of interest	ROI	A continuous portion of an n D continuum. Also called a ‘volume of interest’ (VOI) in 3D.
Region of interest analysis		*0D analyses conducted on a 0D metric extracted from an ROI. Reference: Brett et al. (2002). Equivalent to ‘volume of interest (VOI) analysis’.
Small volume correction	SVC	A multiple comparisons correction across within-ROI values using (parametric) RFT or a nonparametric alternative. RFT is assumed unless otherwise stated. Reference: SPM12 Manual (FIL Methods Group, Wellcome Trust Centre for Neuroimaging, University College London) http://www.fil.ion.ucl.ac.uk/spm/software/spm12/

Appendix B Field smoothness: FWHM

The full width at half maximum (FWHM) parameter describes the smoothness of 1D random fields. Most precisely, the FWHM specifies the breadth of a Gaussian kernel (Fig.B.1) which, when convolved with uncorrelated (perfectly rough) Gaussian 1D data yields smooth Gaussian 1D fields (Fig.B.2).

Random field theory (RFT) (Adler and Taylor, 2007) uses the FWHM value to describe the probabilistic behavior of smooth fields. The most important probability for classical hypothesis testing is the probability that the random fields will reach a certain height (Friston et al., 2007); setting that probability to $\alpha = 0.05$ yields the critical RFT thresholds depicted in Fig.3 (main manuscript).

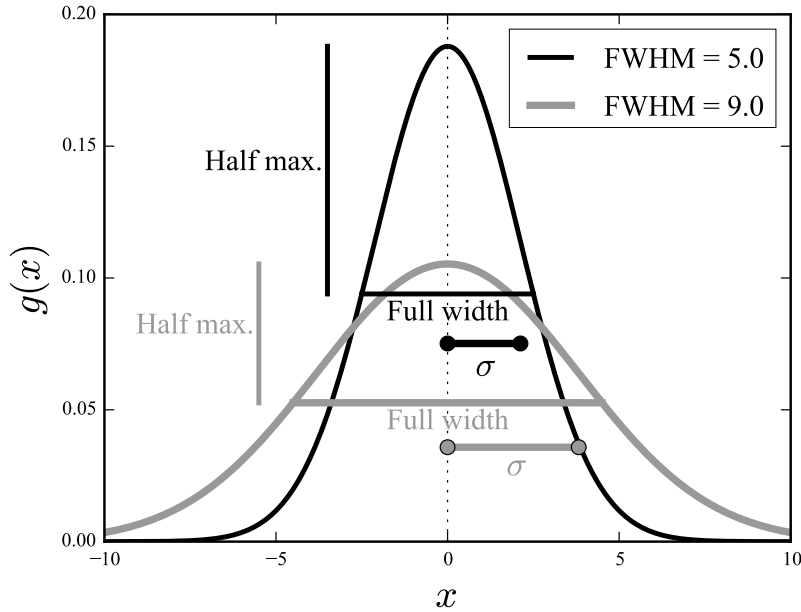


Figure B.1: Breadth parameters for Gaussian kernels: σ and FWHM.

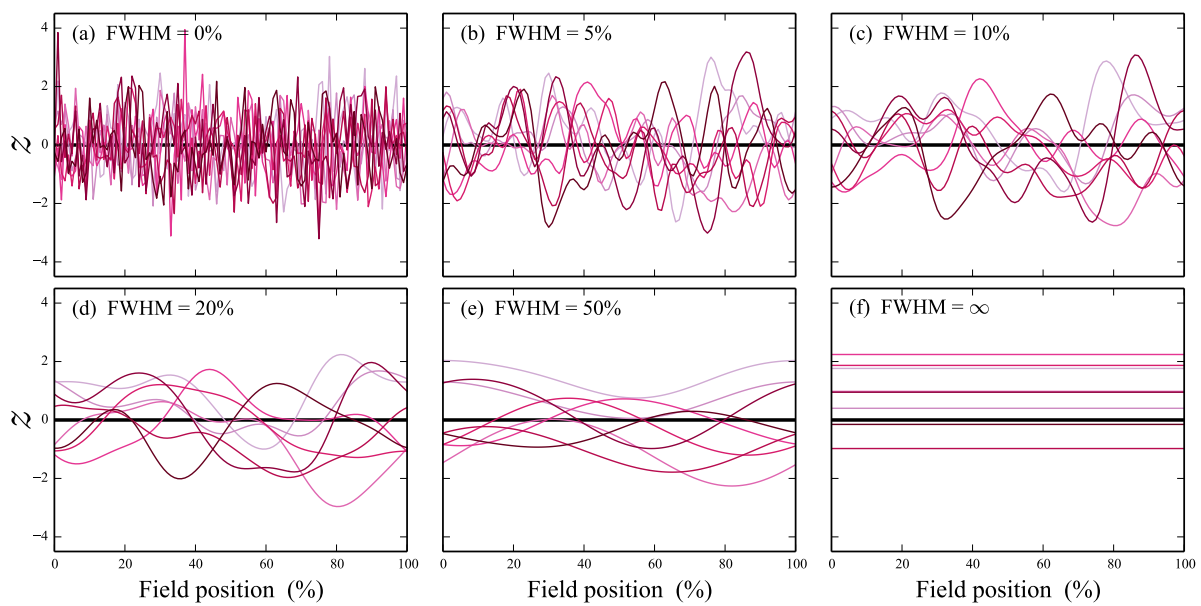


Figure B.2: One-dimensional Gaussian random fields. The FWHM parameterizes field smoothness. The smaller the FWHM the rougher the field, and the more likely random fields are to reach a specified height. Infinitely smooth fields ($\text{FWHM}=\infty$) are probabilistically equivalent to 0D scalars. It has been shown that Biomechanics datasets generally tend to lie in the range $\text{FWHM} = [5\%, 50\%]$, including (processed) kinematics, force and processed EMG (Pataky et al., 2016).

Appendix C ROI analysis in Python and MATLAB

This Appendix describes the Python and MATLAB interfaces for region of interest (ROI) analysis in **spm1d** (www.spm1d.org). Below Python and MATLAB code snippets are presented in green and orange, respectively.

C.1 Example ROI analysis

In **spm1d**, ROI analysis can be conducted using the keyword “roi” in all statistical routines from **spm1d.stats** including t tests, regression, ANOVA, etc. As an example, a two-sample t test with an ROI spanning from time = 10% to 40% can be conducted as follows:

```
import numpy as np
import spm1d

#(0) Load dataset:
YA, YB      = spm1d.data.uv1d.t2.SimulatedTwoLocalMax().get_data()

#(1) Define SR:
roi         = np.array( [False]*101 )
roi[10:40] = True

#(2) Conduct t test:
t           = spm1d.stats.ttest2(YB, YA, roi=roi)
ti          = t.inference(0.05)
ti.plot()
```

```
%(0) Load dataset:
dataset     = spm1d.data.uv1d.t2.SimulatedTwoLocalMax();
[YA, YB]    = deal(dataset.YA, dataset.YB);

%(1) Define ROI:
roi         = false( 1, 101 );
roi(11:40) = true;

%(2) Conduct t test:
t           = spm1d.stats.ttest2(YB, YA, 'roi', roi);
ti          = t.inference(0.05);
ti.plot()
```

C.2 Example analysis in detail

After importing the necessary packages, the next commands retrieve one of spm1d's built-in datasets:

```
YA, YB = spm1d.data.uv1d.t2.SimulatedTwoLocalMax().get_data()
```

```
dataset = spm1d.data.uv1d.t2.SimulatedTwoLocalMax();  
[YA, YB] = deal(dataset.YA, dataset.YB);
```

Here the variables YA and YB are both $(J \times Q)$ arrays, where J and Q are the number of observations and the number of nodes in the 1D continuum, respectively. They can be visualized as follows:

```
from matplotlib import pyplot  
pyplot.plot(YA.T, color="k")  
pyplot.plot(YB.T, color="r")
```

```
plot(YA', 'color','r')  
hold on  
plot(YB', 'color','k')
```

This produces the following figure:

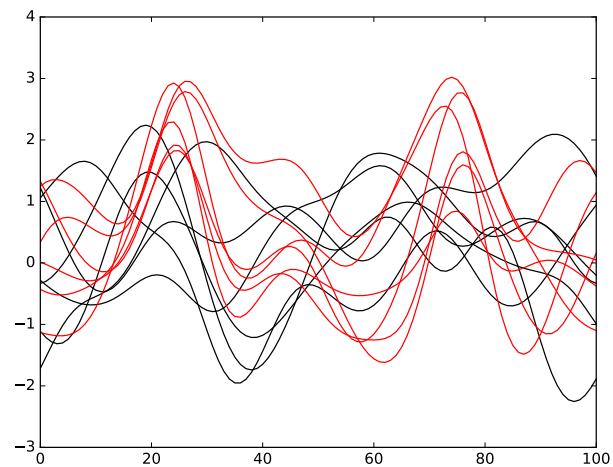


Figure C.1: Example dataset “SimulatedTwoLocalMax”.

In this example the ROI is specified as a binary vector of length Q , where True indicates the ROI:

```
roi = np.array( [False]*101 )  
roi[10:40] = True
```

```
roi      = false( 1, 101 );
roi(11:40) = true;
```

Since the boolean values False and True numerically evaluate to 0 and 1, respectively, the ROI can be visualized using a standard plotting command (Fig.C.2a):

```
pyplot.plot(roi, color="b")
pyplot.ylim(-0.1, 1.1)
```

```
plot(roi, 'color', 'b')
ylim( [-0.1  1.1] )
```

Alternatively the ROI can be visualized using `spm1d`'s "plot_roi" function — currently only available in Python (Fig.C.2b):

```
pyplot.plot(YA.T, color="k")
pyplot.plot(YB.T, color="r")
spm1d.plot.plot_roi(roi, facecolor="b", alpha=0.3)
```

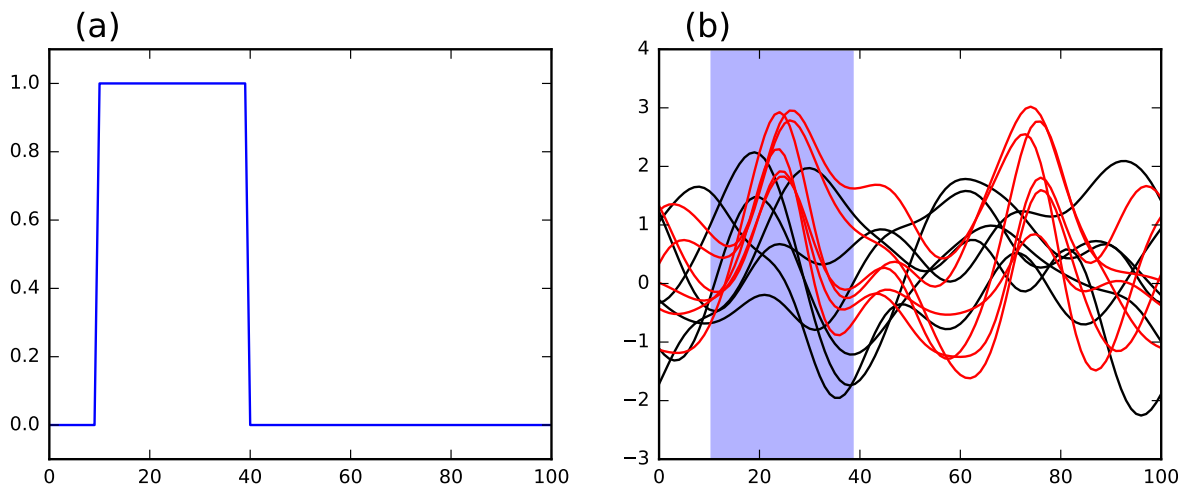


Figure C.2: Example ROI visualization (a) using `pyplot.plot` and (b) using `spm1d.plot.plot_roi`

ROI-based statistical analysis proceeds as follows (Fig.C.3a)

```
t      = spm1d.stats.ttest2(YB, YA, roi=roi)
ti     = t.inference(0.05)
ti.plot()
```



```

0.6659607107024268 1.2186672527052544 1.8786714310449357 2.624090708123374
3.3977458417276942 4.09182563625598 4.557446151350232 4.676118446926481
4.4442233781988865 3.976243703618212 3.414764145392637 2.864043743188491
2.379655562970072 1.9818420780205368 1.6712848172222807 1.4407743903014176
1.2783724255448865 1.17159899332 1.1081081854538306 1.0770125187802424
1.0676148836585948 1.0710020774519424 --- --- --- --- ---
--- --- --- --- ---
--- --- --- --- ---]

```

- Critical thresholds (hashed horizontal lines in Fig.C.3) are always lower in ROI vs. non-ROI analysis because the search volume is smaller.
- When conducting ROI analysis there may be regions outside of the specified ROI which would have reached significance had whole-field analysis been conducted (Fig.C.3b) and/or had the ROIs been chosen differently. This issue is discussed in the main manuscript.

C.3 Multiple ROIs in a single analysis

To conduct statistical analysis using multiple ROIs simply add multiple portions to the boolean vector:

```

roi      = np.array( [False]*101 )
roi[10:40] = True
roi[60:75] = True

```

```

roi      = false( 1, 101 );
roi(11:40) = true;
roi(61:75) = true;

```

When there are multiple ROIs **spm1d** automatically raises the critical threshold to account for the expanded search volume (Fig.C.4). Note that the critical threshold for two ROIs of breadths b_1 and b_2 is not equivalent to the the critical threshold for a single ROI of breadth $(b_1 + b_2)$. For example, using the two-ROIs defined above yields a critical threshold of $t^*=3.115$. If, instead a single ROI of the same total breadth had been defined as follows:

```

roi      = np.array( [False]*101 )
roi[10:55] = True

```

```

roi      = false( 1, 101 );
roi(11:55) = true;

```

the critical threshold would be slightly lower: $t^*=3.050$. The reason is that within-ROI variance is smooth (across the 1D continuum), but between-ROI variance is generally not smooth. The **spm1d** software accounts for this using the Euler characteristic of the specified ROI (see Pataky 2016).

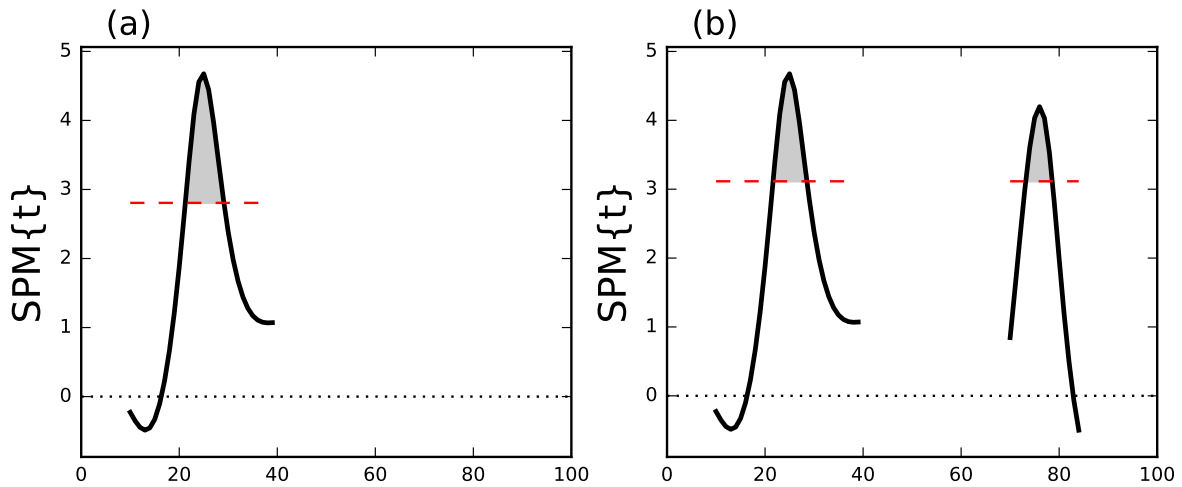


Figure C.4: Example analysis (a) with one ROI and (b) with two ROIs.

C.4 Directional ROIs

‘Directional ROIs’ can be used to simultaneously test a set of one-tailed hypotheses. As depicted in Fig.5 (main manuscript), different ROIs can embody one-tailed hypotheses. Directional ROIs are specified in **spm1d** as an integer vector containing the values: -1, 0 and +1 as follows:

```
roi = np.array( [0]*101 )
roi[10:40] = +1
roi[60:75] = -1
```

```
roi = zeros( 1, 101 );
roi(11:40) = +1;
roi(61:75) = -1;
```

Results for this particular set of directional ROIs as applied to the dataset above are depicted in Fig.C.5b. Interpreting this result is somewhat complex and warrants discussion. First let us compare this result with the case where both ROIs are positive (Fig.C.5a):

```
roi = np.array( [0]*101 )
roi[10:40] = +1
roi[60:75] = +1
```

```
roi = zeros( 1, 101 );
roi(11:40) = +1;
roi(61:75) = +1;
```

There are two results to consider:

1. *Omnibus result*: The omnibus result involves simultaneous testing of all ROIs. In this example there is sufficient evidence to reject the omnibus null hypothesis for both Fig.C.5a and C.5b because the $SPM\{t\}$ crosses the critical threshold in the predicted direction in both cases.
2. *Individual ROI results*: These results may be regarded as a *post hoc* qualification of the omnibus test, much in the same way *post hoc* t tests work in ANOVA. In Fig.C.5a the null hypotheses are rejected for both ROIs, but in Fig.C.5b the null hypothesis is rejected only for the first ROI.

In other words, there is sufficient evidence to reject the omnibus null hypothesis for both Fig.C.5a and Fig.C.5b. In Fig.C.5a there is sufficient evidence to reject the null hypotheses pertaining to both individual ROIs in *post hoc* analysis. However, in Fig.C.5a there is only sufficient evidence to reject the null hypothesis pertaining to the first ROI.

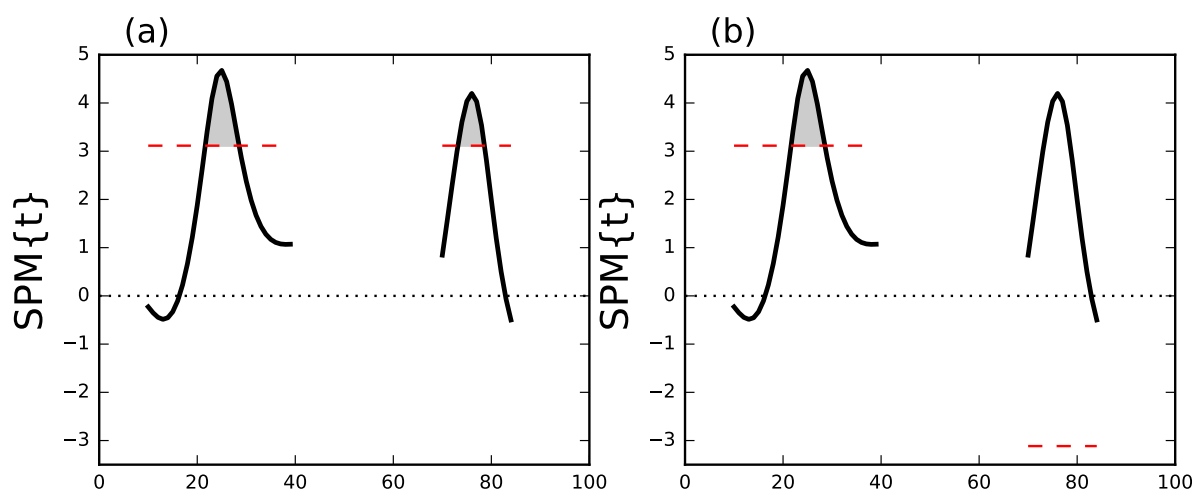


Figure C.5: Example directional ROI analysis. (a) Both ROIs are positive-directed. (b) The first and second ROIs are positive- and negative-directed, respectively.

Appendix D Accessing datasets

All datasets analyzed in this paper are available in the **spm1d** software package (www.spm1d.org) and can be accessed via the **spm1d.data** interface as described below. Python and MATLAB code snippets appear in green and orange font, respectively.

All datasets in **spm1d.data** are organized as follows:

```
spm1d.data.XXXX.ZZZZ.DatasetName
```

where XXXX refers to the data modality (e.g. univariate, one-dimensional), ZZZZ refers to the original or appropriate statistical test (e.g. one-sample t test), and DatasetName is a unique name assigned to each dataset, containing the main author's family name and publication year where appropriate.

Datasets A and B (Pataky et al., 2015)

Datasets A and B contain univariate, one-dimensional data (“uv1d”), the appropriate test for both is a one-sample t-test (“t1”), and the dataset names are “SimulatedPataky2015a” and “SimulatedPataky2015b”. They can be accessed as indicated below. The YA and YB variables are both (10 x 101) arrays, where 10 is the number of responses and 101 is the number of time nodes used to approximate the continuum.

```
import spm1d
datasetA = spm1d.data.uv1d.t1.SimulatedPataky2015a()
datasetB = spm1d.data.uv1d.t1.SimulatedPataky2015b()
YA = datasetA.Y
YB = datasetB.Y
```

```
datasetA = spm1d.data.uv1d.t1.SimulatedPataky2015a();
datasetB = spm1d.data.uv1d.t1.SimulatedPataky2015b();
YA = datasetA.Y;
YB = datasetB.Y;
```

Dataset C (Neptune et al., 1999)

Dataset C contains multivariate, one-dimensional data (“mv1d”), the appropriate test is a paired Hotellings T^2 test (“hotellings paired”), and the dataset name is “Neptune1999kneekin”. They can be accessed as indicated below. The YA and YB variables are both (8 x 101 x 3), where 8 is the number of responses, 101 is the number of time nodes, and 3 is the number of vector components. Although

these data are multivariate, in this study univariate analyses were conducted on only the first vector component (variables yA and yB).

```
import spm1d
dataset = spm1d.data.mv1d.hotellings_paired.Neptune1999kneekin()
YA, YB = dataset.YA, dataset.YB
yA, yB = YA[:, :, 0], YB[:, :, 0]
```

```
dataset = spm1d.data.mv1d.hotellings_paired.Neptune1999kneekin();
[YA, YB] = deal( dataset.YA, dataset.YB );
[YA, YB] = deal( YA(:, :, 1), YB(:, :, 1) );
```

Dataset D (Pataky et al., 2008)

Dataset D contains univariate, one-dimensional data (“uv1d”), the appropriate test is one-way ANOVA (“anova1”), and the dataset name is “SpeedGRFcategory”. Individual subjects’ data can be loaded using the “subj” keyword as indicated below. The Y and A variables in each dataset are (60 x 101), and (60 x 1), respectively, where 60 is the number of responses and 101 is the number of time nodes. Y contains the GRF data and A contains a vector of condition labels, where the labels “1”, “2”, and “3” refer to slow, normal and fast walking, respectively. Note that 20 repetitions of each condition were conducted and that the conditions were presented in a randomized order. In this paper only the normal and fast conditions were considered.

The Y00 and Y01 variables are both (20 x 101) and were used in the Stage 1 analyses (Fig.6a). The Y0 and Y1 variables are both (6 x 101) and contain within-subject mean trajectories for each of the six subjects, and were used in the State 2 analyses (Fig.6b–c).

```
# load pilot subject's data:
subj0 = 0
dataset = spm1d.data.uv1d.anova1.SpeedGRFcategory(subj=subj0)
Y, A = dataset.Y, dataset.A
Y00 = Y[A==2]
Y01 = Y[A==3]

# load experiment subjects' data:
SUBJ = [2, 3, 4, 5, 6, 7]
Y0 = []
Y1 = []
for subj in SUBJ:
    dataset = spm1d.data.uv1d.anova1.SpeedGRFcategory(subj=subj)
    Y, A = dataset.Y, dataset.A
    Y0.append( Y[A==2].mean(axis=0) )
    Y1.append( Y[A==3].mean(axis=0) )
Y0, Y1 = np.array(Y0), np.array(Y1)
```

```

% load pilot subject's data:
subj0      = 0;
dataset    = spm1d.data.uv1d.anova1.SpeedGRFcategoryal(subj0);
[Y,A]      = deal( dataset.Y, dataset.A );
Y00        = Y(A==2,:);
Y01        = Y(A==3,:);

% load experiment subjects' data:
SUBJ       = [2 3 4 5 6 7];
Y0         = zeros(6, 101);
Y1         = zeros(6, 101);
for i = 1:6
    dataset = spm1d.data.uv1d.anova1.SpeedGRFcategoryal( SUBJ(i) );
    [Y,A]    = deal( dataset.Y, dataset.A );
    Y0(i,:)  = mean( Y(A==2,:), 1);
    Y1(i,:)  = mean( Y(A==3,:), 1);
end

```

References

- Adler, R. J. and Taylor, J. E. (2007). *Random Fields and Geometry*. Springer-Verlag.
- Brett, M., Anton, J. L., Valabregue, R., and Poline, J. B. (2002). Region of interest analysis using the marsbar toolbox for spm 99. *NeuroImage*, 16(2):S497.
- Friston, K. J., Ashburner, J. T., Kiebel, S. J., Nichols, T. E., and Penny, W. D. (2007). *Statistical Parametric Mapping: The Analysis of Functional Brain Images*. Elsevier/Academic Press, Amsterdam.
- Neptune, R. R., Wright, I. C., and van den Bogert, A. J. (1999). Muscle coordination and function during cutting movements. *Medicine & Science in Sports & Exercise*, 31(2):294–302, data: <http://isbweb.org/data/rrn/>.
- Pataky, T. C., Caravaggi, P., Savage, R., and Crompton, R. H. (2008). Regional peak plantar pressures are highly sensitive to region boundary definitions. *Journal of Biomechanics*, 41(12):2772–2775.
- Pataky, T. C., Vanrenterghem, J., and Robinson, M. A. (2015). Zero- vs. one-dimensional, parametric vs. non-parametric, and confidence interval vs. hypothesis testing procedures in one-dimensional biomechanical trajectory analysis. *Journal of Biomechanics*, 48(7):1277–1285.
- Pataky, T. C., Vanrenterghem, J., and Robinson, M. A. (2016). The probability of false positives in zero-dimensional analyses of one-dimensional kinematic, force and emg trajectories. *Journal of Biomechanics*, 49:1468–1476.